

Effects of magnetic dipole-dipole interactions in atomic Bose-Einstein condensates with tunable s -wave interactions

Abraham J. Olson,^{*} Daniel L. Whitenack, and Yong P. Chen[†]*Department of Physics, Purdue University, West Lafayette, Indiana 47907, USA*

(Received 6 September 2013; published 8 October 2013)

The s -wave interaction is usually the dominant form of interactions in atomic Bose-Einstein condensates (BECs). Recently, Feshbach resonances have been employed to reduce the strength of the s -wave interaction in many atomic species. This opens the possibilities to study magnetic dipole-dipole interactions (MDDIs) in BECs, where the novel physics resulting from long-range and anisotropic dipolar interactions can be explored. Using a variational method, we study the effect of MDDIs on the statics and dynamics of atomic BECs with tunable s -wave interactions for a variety of species, including both nonalkali metals with large magnetic dipole moments (^{52}Cr , ^{164}Dy , ^{168}Er) and alkali metals (with much smaller magnetic dipole moments). A parameter of magnetic Feshbach resonances, $\epsilon_{dd,\text{max}}$, is used to quantitatively indicate the feasibility of experimentally observing MDDI effects in different atomic species. We find that strong MDDI effects should be observable in both in-trap and time-of-flight behaviors, not only for the strongly magnetic dipolar species but also for the alkali-metal BECs of ^7Li , ^{39}K , and ^{133}Cs . In addition, we predict several effects which should be experimentally observable. Our results provide a helpful guide for experimentalists to realize and study atomic dipolar quantum gases.

DOI: [10.1103/PhysRevA.88.043609](https://doi.org/10.1103/PhysRevA.88.043609)

PACS number(s): 03.75.-b, 67.85.Bc, 67.85.De

I. INTRODUCTION

The physics of ultracold dipolar quantum gases is a rich and promising area of research. There is great interest in the physical behaviors that result from dipole-dipole interactions [1,2]. An ultracold atomic gas of atoms that possess a magnetic moment will have a magnetic dipole-dipole interaction (MDDI). However, it is often difficult to observe the effects of an MDDI in many atomic species (particularly alkali metals), where the MDDI is typically much weaker than the isotropic, s -wave interactions. For atomic species with magnetic Feshbach resonances, however, the s -wave scattering length a_s can be tuned via magnetic fields [3,4]. Employing Feshbach resonances has led to fruitful and impressive developments in ultracold atom research. Of interest here is that it allows for the exploration of MDDIs in Bose-Einstein condensates (BECs). By tuning a_s to near zero, the MDDI can become the strongest interaction in the BEC.

The effect of MDDIs in ultracold atomic gases was first observed using a BEC of ^{52}Cr atoms, which possess a strong magnetic moment μ of 6 Bohr magnetons (μ_B) [5]. The MDDIs were observed to affect the aspect ratio of the ^{52}Cr BEC in time-of-flight (TOF) free expansion. The MDDI effect on the stability of a BEC was also experimentally studied in ^{52}Cr , where for various trap configurations the MDDI either made the BEC more or less stable against collapse [6]. More recently, in ^7Li , the MDDI effect was seen when comparing the axial length of the BEC near $a_s = 0$ for two different trapping geometries [7]. Effects of MDDIs have also been observed on the decoherence rate in a ^{39}K BEC atomic interferometer [8] and on the spin domains of a spinor ^{87}Rb Bose gas [9]. Very recently, a BEC has been realized with ^{164}Dy , with a strong magnetic moment of $10\mu_B$, exhibiting dipolar effects even with no tuning of the scattering length [10].

A strongly magnetic dipolar BEC with a Feshbach resonance tunable s -wave interaction has also been realized in ^{168}Er [11]. Many further effects due to MDDIs have been predicted, such as the excitation of collective modes by tuning the dipolar interaction [12], the emergence of a biconcave structure with local collapse [13,14], and the modification of the phase diagram of dipolar spin-1 BECs [15–17], of the soliton stability in 1D BECs [18], and of vortices in BECs [19]. We refer the reader to recent reviews for a further discussion of the multiplicity of MDDI effects [1,2].

Motivated by such rich physics, we theoretically model the effects of MDDIs and possibility of experimentally detecting such effects in BECs of strongly magnetic dipolar species (^{52}Cr , ^{164}Dy , ^{168}Er) and all the alkali metals. In Sec. II, we explain the variational method we employ to model MDDIs using a computationally efficient, cylindrically symmetric, Gaussian ansatz for the BEC wave function [20]. In Sec. III, we start by discussing the relevant parameters for our simulations. We also introduce a key quantity used in this paper, i.e., the ratio of s -wave scattering length a_s to a length defined for MDDI, a_{dd} . Next in that section we present simulations of the effects of MDDIs in ^{52}Cr , including those reported in Refs. [6,21], and predict several other MDDI signatures that should be readily observable, such as the possibility for collapse after release from a trapping potential. In addition, we present simulations for the effects of MDDIs in ^7Li , ^{39}K , and ^{133}Cs , i.e., the three alkali-metal BECs that we identified as promising for observing MDDI effects. Motivated by the recent achievement of BECs of ^{164}Dy [10] and ^{168}Er [11], we also present calculations of MDDI effects in those highly dipolar atomic species. In Sec. IV, we conclude.

II. VARIATIONAL METHOD

While a few other methods exist to model dipole-dipole interaction effects in BECs [1,22–25], the variational method we employ has shown great utility because its simple,

^{*}olsonaj@purdue.edu[†]yongchen@purdue.edu

analytic solutions are valid over a wide range of experimental parameters [20,26,27]. Two types of interactions are considered. The s -wave interaction is characterized by the s -wave scattering length a_s and, for dipole-dipole interactions, a parameter defined as a_{dd} is used. MDDIs can be characterized by $a_{dd} = \mu_0 \mu^2 M / (12\pi \hbar^2)$, where μ is the magnetic moment of the atom, M is its mass, and μ_0 is the permeability of free space [28]. The atom-atom interaction potential thus has two terms, one for each interaction:

$$V_{\text{atom-atom}}(\vec{R}) = a_s \frac{4\pi \hbar^2}{M} \delta(\vec{R}) + a_{dd} \frac{3\hbar^2}{M} \frac{1 - 3\cos^2\theta}{R^3}. \quad (1)$$

Using that interaction term, the Gross-Pitaevskii equation for a BEC takes the form (in dimensionless units)

$$i \frac{\partial \psi(\vec{r})}{\partial t} = -\frac{1}{2} \nabla^2 \psi(\vec{r}) + V_{\text{ext}}(\vec{r}) \psi(\vec{r}) + \frac{4\pi N a_s}{a_r} |\psi(\vec{r})|^2 \psi(\vec{r}) + \frac{N a_{dd}}{3a_r} \int \frac{1 - 3\cos^2\theta}{R^3} |\psi(\vec{r}')|^2 d\vec{r}' \psi(\vec{r}), \quad (2)$$

where the length unit is $a_r = \sqrt{\hbar/m\omega_r}$, the trap frequencies are ω_r and ω_z for the respective radial and axial direction, the time unit $t = 2\pi/\omega_r$, ψ is normalized to unity ($|\psi|^2 = 1$), and $V_{\text{ext}}(\vec{r}) = \frac{1}{2}(x^2 + y^2 + \lambda^2 z^2)/2$ is the trap potential where the trap aspect ratio is $\lambda = \omega_z/\omega_r$. For this paper, we adopt the nomenclature for trap shapes that is common to experiments: the symmetrical also known as spherical ($\lambda = 1$), the cigar also known as prolate ($\lambda < 1$), and the pancake also known as oblate ($\lambda > 1$) shapes [6]; we also assume that the magnetic field is applied along the axial direction. Using a cylindrical-symmetric, Gaussian ansatz for the BEC wave function [29],

$$\psi(\vec{r}) = \exp\left(-\frac{x^2}{2q_r^2}\right) \exp\left(-\frac{y^2}{2q_r^2}\right) \exp\left(-\frac{z^2}{2q_z^2}\right), \quad (3)$$

the variational method results in two differential equations that describe the mean axial q_z and radial q_r lengths of the BEC (detailed solution in Ref. [20], noting [30]):

$$\ddot{q}_r + q_r = \frac{1}{q_r^3} - \sqrt{\frac{2}{\pi}} \frac{1}{q_r^3 q_z} \frac{N}{a_r} [a_{dd} f(\kappa) - a_s], \quad (4a)$$

$$\ddot{q}_z + \lambda^2 q_z = \frac{1}{q_z^3} - \sqrt{\frac{2}{\pi}} \frac{1}{q_r^2 q_z^2} \frac{N}{a_r} [a_{dd} g(\kappa) - a_s], \quad (4b)$$

where

$$q_r \equiv \sqrt{\frac{\langle x^2 \rangle}{2}} \equiv \sqrt{\frac{\langle y^2 \rangle}{2}}, \quad (5a)$$

$$q_z \equiv \sqrt{\frac{\langle z^2 \rangle}{2}}, \quad (5b)$$

$$\kappa \equiv q_r/q_z, \text{ i.e., the BEC aspect ratio,} \quad (5c)$$

$$f(\kappa) \equiv \frac{[-4\kappa^4 - 7\kappa^2 + 2 + 9\kappa^4 H(\kappa)]}{2(\kappa^2 - 1)^2}, \quad (5d)$$

$$g(\kappa) \equiv \frac{[-2\kappa^4 + 10\kappa^2 + 1 - 9\kappa^2 H(\kappa)]}{(\kappa^2 - 1)^2}, \quad (5e)$$

$$H(\kappa) \equiv \frac{\tanh^{-1}(\sqrt{1 - \kappa^2})}{\sqrt{1 - \kappa^2}}. \quad (5f)$$

TABLE I. Parameters for variational computations, with the maximum value of ϵ_{dd} as calculated from Eq. (6).

Species	$ F, m_F\rangle$	$\mu_{\text{cross}}/\mu_B^a$	$a_{s,\text{min}}(a_0)$	$a_{dd}(a_0)$	$\epsilon_{dd,\text{max}}$
^7Li	$ 1, +1\rangle$	0.94	0.0007	0.041	58.4
^{23}Na	$ 1, +1\rangle$	0.91	0.572	0.047	0.08
^{39}K	$ 1, +1\rangle$	0.95	0.0022	0.287	130
^{41}K	$ 1, -1\rangle$	0.07	0.104	0.002	0.02
^{85}Rb	$ 2, -2\rangle$	-0.57	0.067	0.223	3.33
^{87}Rb	$ 1, +1\rangle$	0.73	5.98	0.374	0.06
^{133}Cs	$ 3, -3\rangle$	-0.75	0.0096	0.607	63.2
^{52}Cr	$ 3, -3\rangle$	6	0.473	15.2	32.2

^aCalculated at B_0 .

These coupled differential equations model BEC behavior with (keeping a_{dd}) and without (setting $a_{dd} = 0$) MDDI effects, and they can be numerically solved to model three experimentally relevant situations:

- (1) The static, *in situ* sizes for a trapped BEC are found by setting the time-dependent components, \dot{q}_r and \dot{q}_z , to zero.
- (2) In-trap dynamics are modeled by keeping all terms.

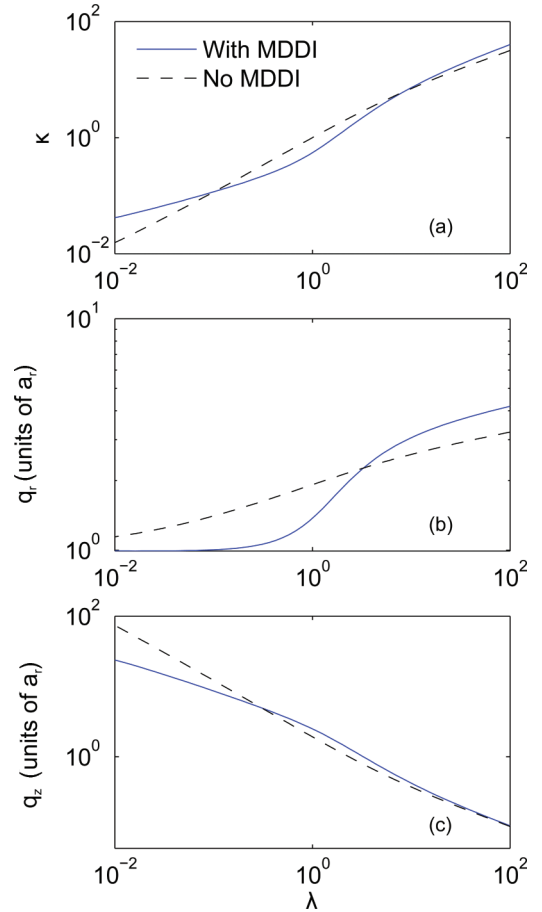


FIG. 1. (Color online) The calculated in-trap BEC (a) aspect ratio, (b) radial length, and (c) axial length of a ^{52}Cr BEC with (solid blue line) and without (dashed black line) MDDIs for a range of trap aspect ratios, λ . In this simulation, $f_{\text{avg}} = 700$ Hz, atom number $N = 2 \times 10^4$, and $a_s = 15a_0$. The magnetic field is, as for all simulations in this paper, aligned along the axial direction.

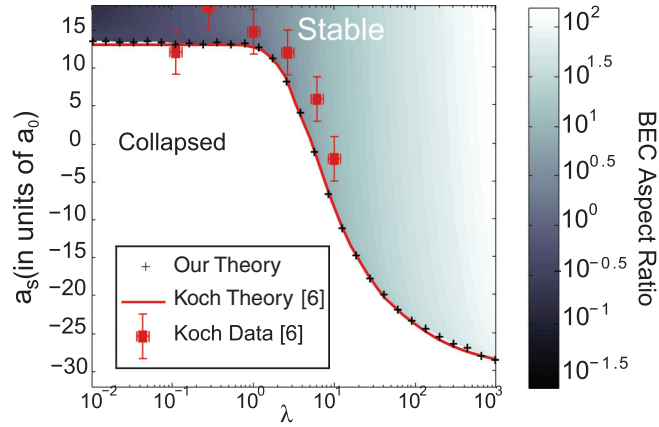


FIG. 2. (Color online) Stability diagram and aspect ratio of a ^{52}Cr BEC, with parameters ($f_{\text{avg}} = 700$ Hz and $N = 2 \times 10^4$) chosen to resemble those in the experiment in Ref. [6]. The BEC aspect ratio κ , solved using our method, is plotted in the color map as functions of a_s and λ in the stable regime (logarithmic scale). The energy variational solution and experimental data from Ref. [6] for $a_s^{\text{threshold}}$ are included for comparison. This shows the effectiveness of our method in solving not just the $a_s^{\text{threshold}}$ where the BEC collapses, but also the BEC size in the stable regime.

(3) Time-of-flight (TOF) free expansion behavior is modeled by removing the terms q_r and $\lambda^2 q_z$, which represent the trapping potential, on the left sides of Eqs. (4).

III. RESULTS

In this section, we employ the above method to solve for both the in-trap and TOF behaviors of BECs with MDDI [31]. We also find the threshold a_s , denoted $a_s^{\text{threshold}}$, below

which the BEC is unstable and collapses. We benchmark our variational calculations against available experimental results in ^{52}Cr and find good agreement (Sec. III B). We also make predictions of MDDI effects in the alkali metals and find that ^7Li , ^{39}K , and ^{133}Cs are the species most favorable for the exploration of MDDI effects. Finally, we present some simulations of MDDI effects in ^{164}Dy and ^{168}Er BECs, both of which have very strong magnetic dipolar interactions.

A. Parameters

The input parameters used in our simulation are the number of atoms in the trap (N), the magnetic dipole moment of the atom (μ), the mass of the atom (M), the axial (f_z) and radial (f_r) frequencies of the trap ($2\pi f_{r,z} = \omega_{r,z}$), and the s -wave scattering length (a_s). An applied magnetic field can tune a_s via a Feshbach resonance with an analytic approximation given by $a_s(B) = a_{bg}(1 - \frac{\Delta}{B - B_\infty})$, where Δ is the width and B_∞ is the location of the Feshbach resonance, and a_{bg} is the scattering length far from any resonances. An experimental limit for reaching small a_s is the precision of control over the magnetic fields. In typical ultracold atom experiments, an experimental precision $\delta B/B$ of approximately 10^{-5} can be realized [32–34]. As μ depends on the strength of the magnetic field, we calculate μ at $B_0 = B_\infty + \Delta$ (where $a_s = 0$), denoted μ_{cross} . For reference, some parameters for known Feshbach resonances from the literature are listed along with the calculated values of μ_{cross} in Appendix A, Table III.

To compare the potential for experimentally observing MDDI effects in the various atomic species of interest, we employ the dimensionless ratio $\epsilon_{dd} = a_{dd}/a_s$ used in Ref. [21], focusing on its maximal value that can be achieved

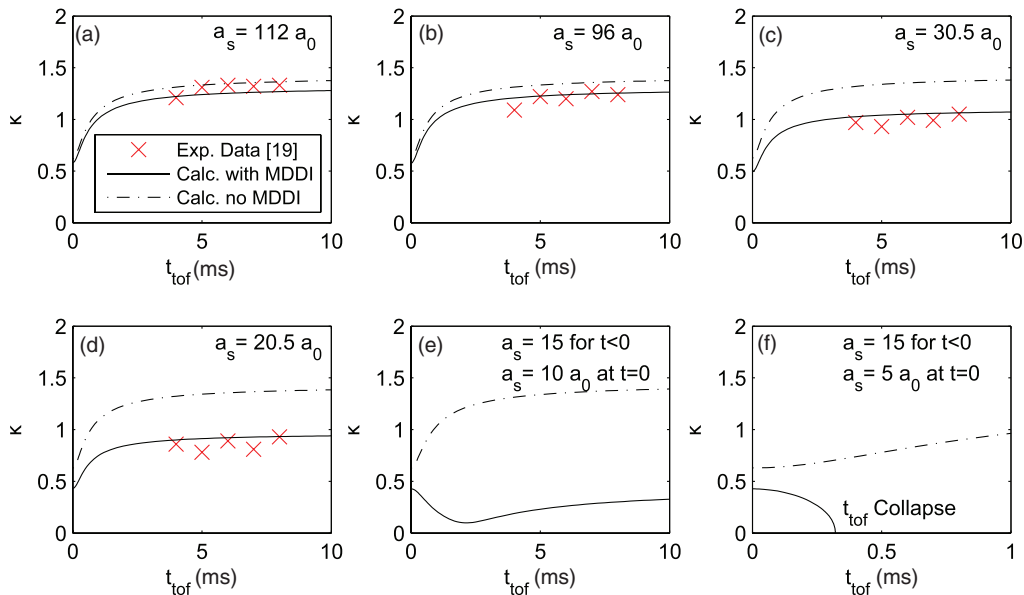


FIG. 3. (Color online) The aspect ratio of a ^{52}Cr BEC vs the time-of-flight duration, t_{TOF} , for different scattering lengths, (a)–(d), with parameters chosen to resemble those in Ref. [21]. We additionally show simulated TOF behavior where the MDDI (e) nearly and (f) actually causes BEC collapse. Upon the release of the BEC, the scattering length is tuned to (e) $a_s = 10 a_0$ and (f) $a_s = 5 a_0$. For (a)–(f), $N = 3 \times 10^4$, $f_r = 600$ Hz, and $f_z = 370$ Hz.

experimentally:

$$\epsilon_{dd, \max} \equiv \frac{a_{dd}}{a_{s, \min}} = \frac{\mu_0 \mu^2 m}{12\pi \hbar^2 a_{bg} (\delta B / \Delta)}, \quad (6)$$

where $a_{s, \min} \approx a_{bg} (\delta B / \Delta)$ is the minimal a_s that can be achieved given a typical experimental magnetic field stability (assumed to be $\delta B / B_0 \approx 10^{-5}$). The alkali-metal species that are the best candidates for observing and studying MDDI effects in BECs are clearly ${}^7\text{Li}$, ${}^{39}\text{K}$, and ${}^{133}\text{Cs}$ (see Table I). We note that ${}^{52}\text{Cr}$, while having a much larger a_{dd} , does not have a broad Feshbach resonance that allows for as precise tuning of a_s , as in some of the alkali metals.

As an initial verification of our model, we compute κ , *in situ* ($t = 0$) and in the TOF asymptotic limit ($t \rightarrow \infty$) assuming only *s*-wave interactions, for both strongly interacting ($a_s \rightarrow$ large) and noninteracting ($a_s = 0$) cases. The expected in-trap and TOF behaviors of a BEC in such limiting cases are (see Refs. [35,36])

- (1) If $a_s = 0$ and $t = 0$, expect $\kappa = \sqrt{\frac{\omega_z}{\omega_r}} = \lambda^{1/2}$.
- (2) If $a_s =$ large and $t = 0$, expect $\kappa = \frac{\omega_z}{\omega_r} = \lambda$.
- (3) If $a_s = 0$ and $t \rightarrow \infty$, expect $\kappa = \sqrt{\frac{\omega_r}{\omega_z}} = \lambda^{-1/2}$.
- (4) If $\lambda \ll 1$ or $\lambda \gg 1$, and if $a_s =$ large with $t \rightarrow \infty$, expect $\kappa = \frac{2}{\pi} \frac{\omega_r}{\omega_z} = 2\lambda^{-1}/\pi$.

Our variational calculation (performed with $\mu = 0$ in these cases) does reproduce these expected values for κ .

B. Effects of MDDIs in ${}^{52}\text{Cr}$ BEC

The first observation of MDDIs in a BEC was with ${}^{52}\text{Cr}$. As ${}^{52}\text{Cr}$ is the most studied atomic species so far for MDDI effects in BECs, we present and benchmark our calculation and results for ${}^{52}\text{Cr}$ before discussing the alkali metals. We used ${}^{52}\text{Cr}$ to demonstrate four types of characteristic MDDI effects, some which have yet to be experimentally explored, discussed in detail below.

1. Effect of MDDIs on *in situ* aspect ratio of a BEC

A calculated result of a ${}^{52}\text{Cr}$ BEC trapped in a harmonic trap is shown in Fig. 1. For a nearly symmetrical trap ($\lambda \approx 1$, which is the case for the experiment in Ref. [6]), the MDDIs increase the axial length of the BEC and reduce its radial length compared to a BEC with no MDDIs, leading to a decreased aspect ratio. However, if the trap is very prolate, $\lambda \ll 1$ (very oblate, $\lambda \gg 1$), we find that the BEC will shrink (expand) in both the axial and radial directions, in a way that leads to an *increased* aspect ratio, which is opposite to the effect previously studied for less anisotropic BECs. There are two values of λ , i.e., one for when the trap is oblate and one for when the trap is prolate, where the MDDIs do not change the aspect ratio of the BEC. Similar *in situ* effects of MDDIs on κ were found in all simulations of stable BECs for the alkali metals as well.

2. Effect of MDDIs on stability of a trapped BEC

For BECs with only *s*-wave interactions, it is shown that if $a_s < 0$ (attractive interactions), then the BEC will collapse if $N \gtrsim 0.55 a_{ho} / |a_s|$, where $a_{ho} = \sqrt{\hbar / m \bar{\omega}}$ and $\bar{\omega}$ is the average trap frequency [36–38]. For any purely *s*-wave interacting BECs held in a three-dimensional harmonic trap, the BEC

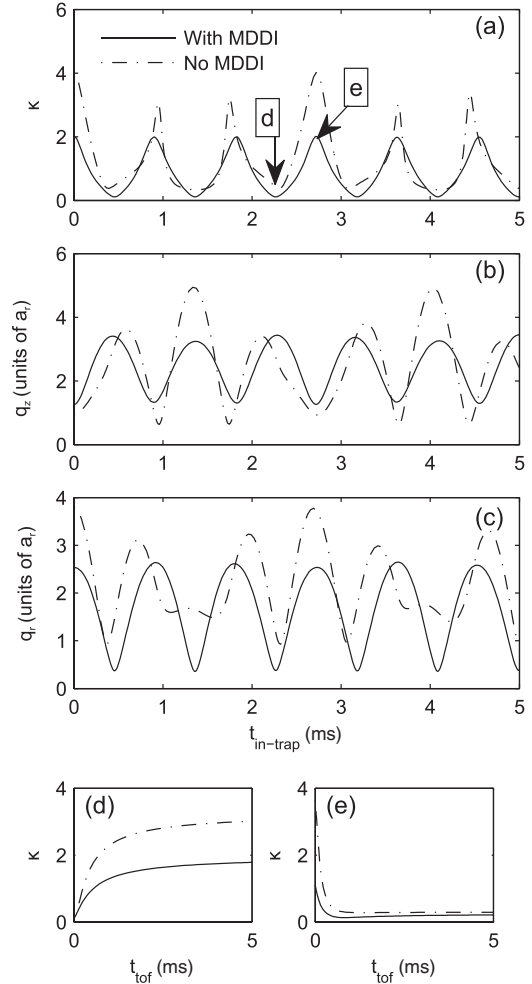


FIG. 4. The (a) aspect ratio, (b) axial length, and (c) radial length for a ${}^{52}\text{Cr}$ BEC evolving in a trap with an initial radial length that is twice the static value and the initial axial length that is half the static value. (d) and (e) show the free expansion for the BEC if it was released at times from the trap when the aspect ratio is at minimum and maximum values, respectively. The release points are indicated with arrows in (a). The parameters used in (a)–(e) are $f_z = f_r = 700$ Hz, $N = 2 \times 10^4$, and $a_s = 14a_0$.

will not collapse if $a_s > 0$. However, MDDIs can destabilize or stabilize a BEC that would otherwise be stable or unstable. The effect of MDDIs on the stability of a trapped BEC was first observed in ${}^{52}\text{Cr}$ [6]. For cigar traps with the *B* field aligned along the axial direction, MDDIs can lead to BEC collapse at a larger value of a_s (in some cases, even $a_s > 0$) than in an otherwise identical BEC with no MDDIs. For pancake traps, the effect is opposite, and the MDDIs stabilize the BEC. Koch *et al.* performed an experimental study of this MDDI effect [6]. To model their results, Koch *et al.* employed an energy argument based on a finding of the energy landscape with q_r and q_z as variational parameters. Differing from their approach, our calculation directly solves for q_r and q_z using Eqs. (4a) and (4b) over a range of a_s , and we find the threshold a_s when those equations do not have a solution, which indicates BEC collapse. This direct method allows not only the determination of the threshold a_s

for collapse (which agrees with those obtained in Ref. [6]), but also the axial and radial BEC lengths over the entire range of a_s where the BEC is stable. As a benchmark, we employed our method using N and f_{avg} identical to those used in Fig. 3 of Ref. [6] to solve for the threshold a_s and also κ for $a_s > a_s^{\text{threshold}}$ over a range of λ (see Fig. 2). We find excellent agreement with both the calculation and experimental data of Koch *et al.* Our calculation shows, as observed in the original experiment [6], that the anisotropic dipole-dipole interactions cause the threshold a_s to depend strongly on the trap geometry. A similar dependence of $a_s^{\text{threshold}}$ on λ is also seen later in this paper for alkali-metal BECs.

3. MDDI effect in time-of-flight behavior

An MDDI affects the behavior of a BEC released from a trap, and such an effect was first observed in an experiment on ^{52}Cr , where the BEC's aspect ratio in TOF changed when the applied magnetic field was along the axial versus radial direction [5,21].

We have simulated the experiment in Ref. [21] (specifically, the data shown in their Fig. 4) and find good agreement. We assume a cylindrically symmetric ($f_r = 600$ and $f_z = 370$ Hz) trap for ease of calculation, with parameters approximating their “trap 2,” which had frequencies $f_x, f_y, f_z = 660, 540, 370$ Hz, respectively, and $N = 3 \times 10^4$. The values of a_s ($112 a_0, 96 a_0, 30.5a_0, 20.5a_0$) and resulting ϵ_{dd} are chosen to match the values in Figs. 4(a)–4(d) of [21] ($\epsilon_{dd} = 0.14, 0.16, 0.5, 0.75$). Even with the cylindrical trap approximation, the simulation results agree with the observed data quite well and clearly show the effect of MDDIs to reduce the aspect ratio of the BEC in TOF from this trap configuration, as shown in Fig. 3. We further show that in the case of small

a_s , MDDI-induced collapse could also be observed after a BEC is released from a trap if the a_s is tuned to a small value upon release. Such a TOF collapse has not been explored, but should be experimentally observable. Figure 3 also shows the MDDI-induced near collapse [Fig. 3(e)] and collapse [Fig. 3(f)] of atoms in free expansion [39].

4. Effect of MDDI on in-trap dynamics

Our model can also solve the in-trap dynamics of BECs with an MDDI. A simulation of the aspect ratio, radial size (q_r), and axial size (q_z) of a trapped ^{52}Cr BEC—initially perturbed from its static state—evolving with time is shown in Fig. 4, revealing an oscillatory behavior. One effect of the MDDI in this situation is to reduce the amplitude of the oscillations. The oscillations may be difficult to observe *in situ* due to the small condensate size, but would become easier to observe in TOF measurements taken from different instants of the oscillations. As seen in Figs. 4(d) and 4(e), the aspect ratio in the TOF changes by a factor of about 2 because of the MDDI. An in-depth treatment of the modes of oscillatory, in-trap dynamics of a BEC with an MDDI can be found in Refs. [40,41].

MDDI effects have been observed in collective oscillations of ^{52}Cr BECs [42]. While the results of Ref. [42] cannot be directly simulated by our method because their magnetic field was not aligned on the axial direction of the BEC, we are motivated by this experiment to study the collective oscillations of BECs with MDDI. By taking the Fourier transform of the time-dependent, in-trap oscillations, we obtain the frequency spectra of the collective oscillations of a BEC with MDDI, exemplified in Fig. 5. The three lowest modes of oscillation were observed, and shifts due to

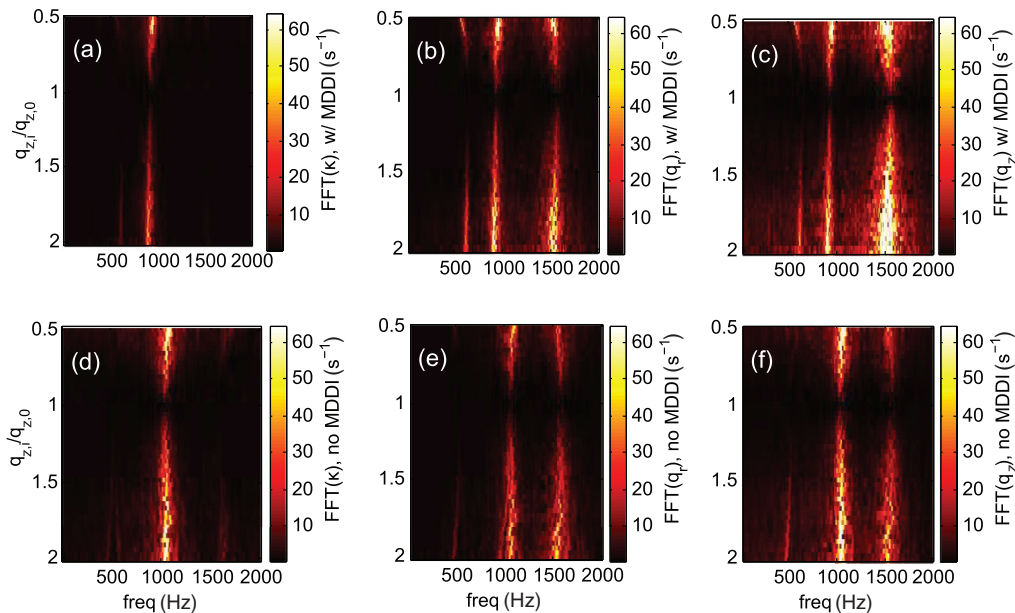


FIG. 5. (Color online) Simulation of a ^{52}Cr BEC frequency spectra of the in-trap oscillations. Frequency spectra are obtained by taking the Fourier transform of the in-trap oscillations of the (a) and (d) aspect ratio κ , (b) and (e) radial length q_r , and (c) and (f) axial length q_z that occur after changing the axial size to $q_{z,i}$ from its in-trap equilibrium value $q_{z,0}$. The color bar gives the amplitude of the fast Fourier transform (FFT) for each plot. Note the shifts in both amplitude and frequency of oscillations between the simulations (a)–(c) including and (d)–(f) not including MDDI. The parameters assumed a spherical trap with $f_r = f_z = 700$ Hz, $N = 2 \times 10^4$, and $a_s = 14a_0$.

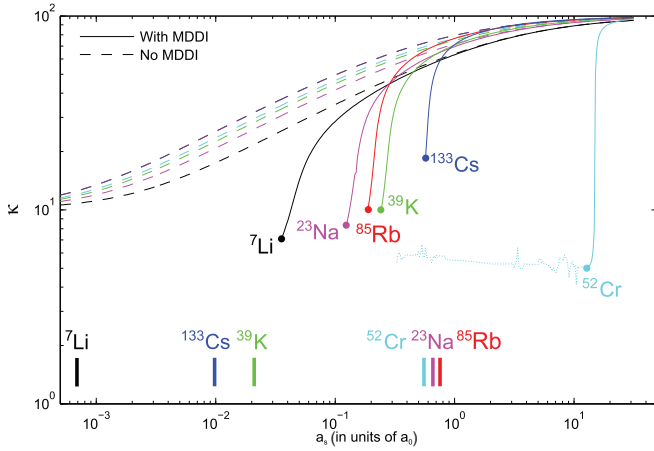


FIG. 6. (Color online) The in-trap aspect ratio for a BEC near $a_s = 0$. The colored, vertical bars indicate the minimum scattering length currently achievable in typical experiments, $a_{s,\min}$. Calculation for each species assumes a cigar trap with $\lambda = 100$ where $f_z = 20$ Hz, $f_r = 2000$ Hz, and 10^6 atoms in the BEC. A thick dot at the end of each solid curve indicates the $a_s^{\text{threshold}}$, which depends both on the mass and the magnetic moment of the atom. The dotted line, shown only for ^{52}Cr as a demonstrative example, indicates the numerically unstable solutions for $a_s < a_s^{\text{threshold}}$ and is used to determine the threshold a_s . Collapse threshold values from the smallest to largest are 0.03, 0.12, 0.19, 0.24, 0.54, $13.50 \times a_0$ for ^7Li , ^{23}Na , ^{85}Rb , ^{39}K , ^{133}Cs , ^{52}Cr , respectively.

MDDI were seen in both the amplitude and frequency of the modes.

C. Results for alkali metals

1. Highlight of MDDI effects in alkali-metal BECs: Stability

A central point of our paper is that MDDI effects are also possible to observe in BECs of the alkali metals, even with a much smaller μ than ^{52}Cr . To show this, we compare dipolar collapse for BECs of various species in Fig. 6. If the MDDIs are not included in the model, then the BECs are stable for any positive value of a_s . However, with MDDIs, the BEC aspect ratio decreases more substantially as a_s is reduced towards zero. The BEC collapses beyond a $a_s^{\text{threshold}}$, indicated by the heavy dot. The value of $a_s^{\text{threshold}}$ can be compared with the $a_{s,\min}$ of Table I, indicated by the color bars in the figure. This comparison clearly indicates whether the observation of collapse due to MDDIs is feasible with current experimental abilities and reveals ^7Li , ^{39}K , and ^{133}Cs as promising alkali-metal species for such an observation.

2. ^7Li , ^{39}K , and ^{133}Cs

We find that ^7Li , ^{39}K , and ^{133}Cs possess the greatest potential among alkali-metal BECs for exploring MDDI effects. Several examples of such effects are shown in the simulations below. We describe ^7Li in detail, and similar results are presented for ^{39}K and ^{133}Cs . The $|1, +1\rangle$ state of ^7Li is excellent for studying MDDI effects as it has the widest known Feshbach resonance of the alkali-metal atoms; the slope at zero crossing is only $\approx 0.1a_0/G$ [7]. Using our variational method, we find that each of the MDDI effects discussed so

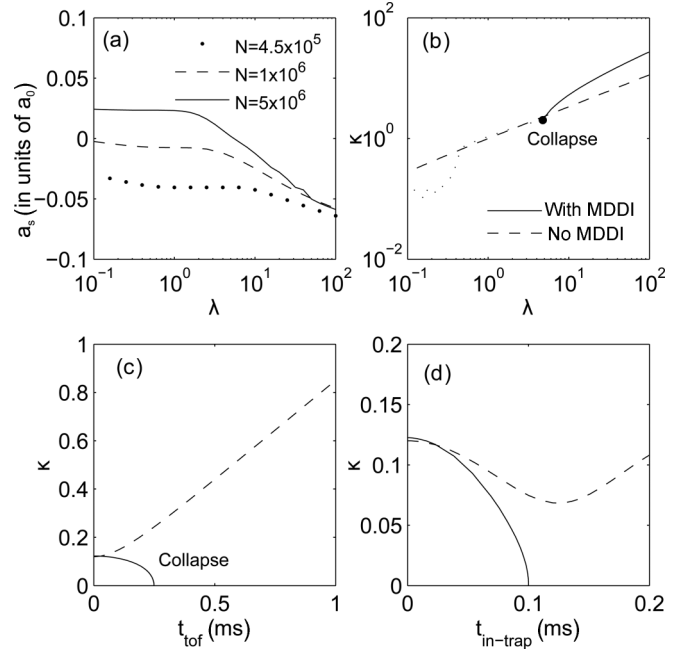


FIG. 7. Effect of an MDDI in a ^7Li BEC. (a) The calculated threshold a_s between stable and unstable regimes for a range of λ and three representative atom numbers. (b) The BEC aspect ratio over a range of λ , with the collapse regime indicated by the faint dotted line, for which there is no stable solution found for Eqs. (4a) and (4b). (c) Evolution of the aspect ratio of the BEC in TOF expansion after release from a trap. In the trap, $a_s = 0.1a_0$ (where the BEC is stable) and, upon release, a_s is tuned to $0.001a_0$ to induce collapse in free expansion. (d) The in-trap evolution of a BEC similar to (c) with a_s tuned to $0.001a_0$ at $t = 0$ to induce in-trap dipolar collapse. Parameters used in the simulation: (a) and (b) $f_{\text{avg}} = 700$ Hz; (b) $N = 5 \times 10^6$ and $a_s = 0.001a_0$; (c) and (d) $f_z = 200$ Hz and $f_r = 2000$ Hz with $N = 5 \times 10^6$.

far in ^{52}Cr should be observable within current experimental capabilities with ^7Li as well.

Figure 7(a) shows the effect of λ and a_s on the stability of a BEC with an MDDI. The line for each simulated BEC atom number N indicates the boundary between the stable (above) and unstable (below) regimes. Similar to the ^{52}Cr case (Fig. 2), the effect of an MDDI is to stabilize a BEC in a pancake trap and to destabilize a BEC in a cigar trap. Figure 7(b) shows κ over a range of λ , with the collapsed regime indicated by the faint, dotted line. Figure 7(c) shows plots of κ after release from a trap. The in-trap starts with $a_s = 0.01a_0$ (in the stable regime) and, upon release (at $t = 0$ in the simulation), a_s is tuned to $0.001a_0$ to induce collapse in free expansion. Such rapid modulation of a_s has already been performed experimentally in ^7Li BECs [43], and here could be used to reveal MDDI effects. Figure 7(d) shows the in-trap evolution of a BEC initially at $a_s = 0.01a_0$ and then tuned to $0.001a_0$ at $t = 0$ to induce in-trap collapse due to MDDI. Neglecting MDDI would result in a stable, oscillating BEC, as seen in Fig. 7(d). The results in Fig. 7 offer four methods for detecting MDDIs in ^7Li BECs. Similar calculations are provided for ^{39}K and ^{133}Cs , as seen in Figs. 8 and 9, respectively. We have shown that the MDDI can have a substantial impact on the shape and stability for each of these alkali-metal BECs.

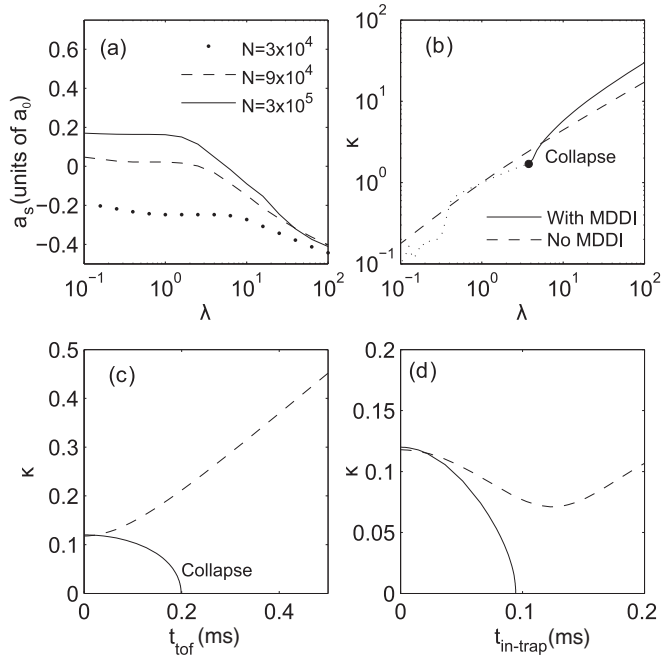


FIG. 8. Effect of an MDDI in a ^{39}K BEC. (a) The calculated threshold a_s between stable and unstable regimes for a range of λ and three representative atom numbers. (b) The BEC aspect ratio over a range of λ , with the collapse regime indicated by the faint dotted line, for which there is no stable solution found for Eqs. (4a) and (4b). (c) Evolution of the aspect ratio of the BEC in TOF expansion after release from a trap. In the trap, $a_s = 0.5a_0$ (where the BEC is stable) and, upon release, a_s is tuned to $0.05a_0$ to induce collapse in free expansion. (d) The in-trap evolution of a BEC similar to (c) with a_s tuned to $0.05a_0$ at $t = 0$ to induce in-trap dipolar collapse. Parameters used in the simulation: (a) and (b) $f_{\text{avg}} = 700$ Hz; (b) $N = 5 \times 10^5$ and $a_s = 0.05a_0$; (c) and (d) $f_z = 200$ Hz and $f_r = 2000$ Hz with $N = 5 \times 10^5$.

3. Other alkali metals

While some of the other alkali metals have the potential for observing the effects of MDDIs, the effects are usually small. For example, in ^{23}Na and ^{85}Rb BECs with atom number and trapping frequencies similar to current experiments (see Table II), a calculation including MDDIs makes a five to ten percent difference in the TOF aspect ratio from a calculation where MDDIs are not included. Thus, although small, the MDDI effect lies within the bounds of possible experimental observations. For ^{41}K and ^{87}Rb , however, the Feshbach resonance is too narrow to provide the precision control of a_s to carry out the type of experiments proposed here, and the MDDI effect is less than a one percent perturbation on the aspect ratio.

D. Results for ^{164}Dy and ^{168}Er

Due to the much higher dipole moments in ^{164}Dy and ^{168}Er ($10\mu_B$ [10] and $7\mu_B$ [11,44], respectively), the effects of MDDIs will be apparent with larger values of a_s than the alkali metals. In Fig. 10, we present similar calculations to those of the alkali metal for these highly magnetic dipolar species, with the collapse dynamics occurring at higher values of a_s .

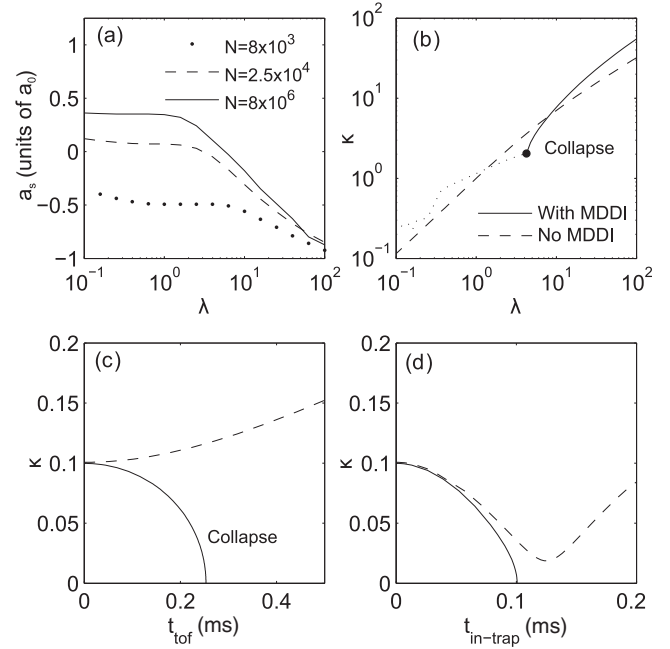


FIG. 9. Effect of an MDDI in a ^{133}Cs BEC. (a) The calculated threshold a_s between stable and unstable regimes for a range of λ and three representative atom numbers. (b) The BEC aspect ratio over a range of λ , with the collapse regime indicated by the faint dotted line, for which there is no stable solution found for Eqs. (4a) and (4b). (c) Evolution of the aspect ratio of the BEC in TOF expansion after release from a trap. In the trap, $a_s = 5a_0$ (where the BEC is stable) and, upon release, a_s is tuned to $0.1a_0$ to induce collapse in free expansion. (d) The in-trap evolution of a BEC similar to (c) with a_s tuned to $0.1a_0$ at $t = 0$ to induce in-trap dipolar collapse. Parameters used in the simulation: (a) and (b) $f_{\text{avg}} = 700$ Hz; (b) $N = 2 \times 10^6$ and $a_s = 0.1a_0$; (c) and (d) $f_z = 200$ Hz and $f_r = 2000$ Hz with $N = 2 \times 10^6$.

IV. CONCLUSION

We showed that the variational method provides a useful and simple tool to simulate the effects of MDDIs in BECs and presented various results for ^{52}Cr , alkali metals, and the strongly magnetic dipolar lanthanides ^{164}Dy and ^{168}Er . For example, examining the the aspect ratio of freely expanding BECs should be sufficient for detecting the effects of MDDIs in many species, and we suggest the investigation of ^7Li , ^{39}K , and ^{133}Cs as favorable to detect such effects in spite of their

TABLE II. An example list of representative parameters for alkali-metal BECs from the literature.

Species	f_r (Hz)	f_z (Hz)	No. of atoms	Ref.
^7Li	193	3	3×10^5	[7]
^{23}Na	1500	150	3×10^5	[45]
^{39}K	65 to 74	92	3×10^4	[46]
^{41}K	325	15	3×10^5	[47]
^{85}Rb	17	6.8	1×10^5	[48]
^{87}Rb	930	11	3.6×10^6	[32]
^{133}Cs	14	14	1.6×10^4	[49]
^{52}Cr	600	370	3×10^4	[21]

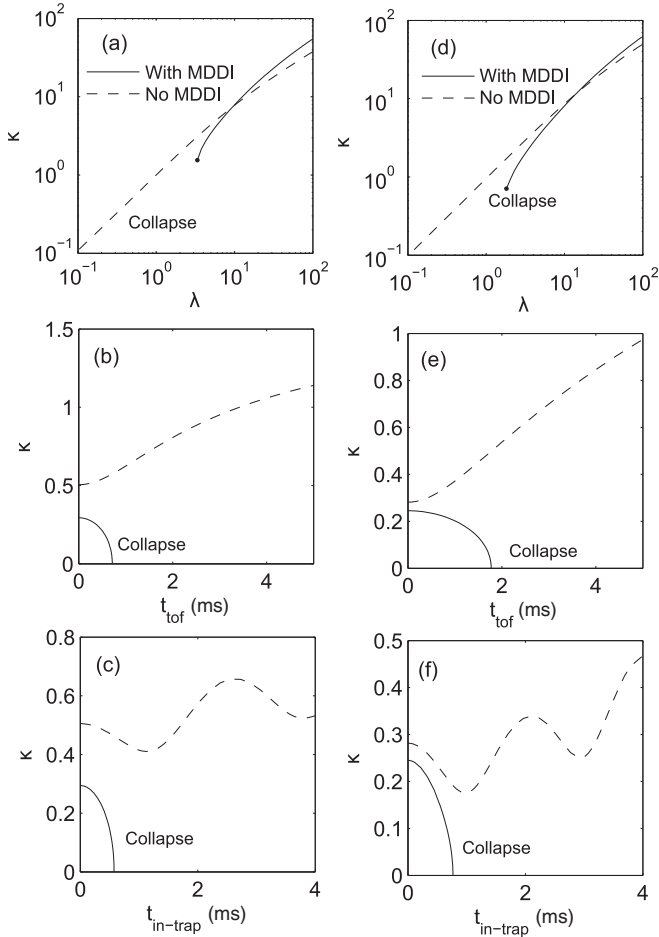


FIG. 10. Effects of MDDIs in ^{164}Dy and ^{168}Er . The left column (a)–(c) contains results for ^{164}Dy and the right column (d)–(f) for ^{168}Er . (a) and (d) The BEC aspect ratio over a range of λ , with the collapse regime indicated by the faint dotted line, for which there are no stable solutions found for Eqs. (4a) and (4b). (b) and (e) Evolution of the aspect ratio of the BEC in TOF expansion after release from a trap. In the trap, $a_s = 150a_0$ (where the BEC is stable for both species) and, upon release, a_s is tuned to $75a_0$ ($50a_0$) for ^{164}Dy (^{168}Er) to induce collapse in free expansion. (c) and (f) The in-trap evolution of a BEC similar to (b) with a_s tuned to $75a_0$ ($50a_0$) for ^{164}Dy (^{168}Er) at $t = 0$ to induce in-trap dipolar collapse. For all ^{164}Dy calculations, $N = 1.5 \times 10^4$, and for all ^{168}Er , $N = 7 \times 10^4$. (a) and (d) $f_{\text{avg}} = 170$ Hz and $a_s = 150a_0$. (b) and (c) $f_z = 100$ Hz and $f_r = 200$ Hz. (e) and (f) $f_z = 70$ and $f_r = 250$ Hz.

relatively small magnetic dipole moments. We mention that future investigation of MDDIs among nonalkali-metal species looks promising as well. The achievement of BECs with ^{164}Dy ($\mu = 10\mu_B$) [10] and ^{168}Er ($\mu = 7\mu_B$) [11] is quite exciting, as the a_{dd} for ^{168}Er and ^{164}Dy are $66.3 a_0$ and $131.5 a_0$, which are much greater than even that of ^{52}Cr . The ability to tune a_s by Feshbach resonance could make these species unparalleled for the observation of strong MDDI effects. To close, we highlight that the effects of an MDDI on the BEC shape provide a clear and intuitive picture of MDDIs in BECs. The examination of the BEC aspect ratio, for example, can be used as a sensitive measurement of the a_s value *in situ*, and may prove to be a helpful calibration method for future studies of other—perhaps more exotic—MDDI effects. We also note that while our discussion is limited to magnetic dipole-dipole interactions in this paper, the variational method we present is general for all dipolar BECs and may be employed in calculating the effects of electric dipole-dipole interactions (e.g., polar molecular BECs) as well [20].

ACKNOWLEDGMENTS

The authors thank R. M. Wilson, R. G. Hulet, Han Pu, Yi Su, and Li You for discussions, and T. Lahaye and T. Koch for providing various data on ^{52}Cr . Y.P.C. acknowledges the support of the Miller Family Foundation and NSF Grant No. CCF-0829918. A.J.O. was supported by the Department of Defense through the National Defense Science and Engineering Graduate (NDSEG) Fellowship Program.

APPENDIX A: SUPPLEMENTAL EXPERIMENTAL PARAMETERS

Typical atom numbers and trap frequencies currently employed in experimental studies of alkali-metal BECs from the literature are listed below to show the experimental feasibility of the simulations provided here (Table II).

APPENDIX B: CALCULATING THE MAGNETIC MOMENT

A key parameter for the variational simulation is the value of the magnetic dipole moment, as $a_{dd} \propto \mu^2$. In low fields, the magnetic moment is found from the Zeeman effect, where

$$\Delta E_{|Fm_F\rangle} = \mu_B g_F m_F B_z. \quad (\text{B1})$$

TABLE III. Various parameters for the atomic species discussed in this paper. Values for g_I are from Ref. [55]. Values for A_{hfs} are from [50]. We use $g_I = 2.002\,319\,304\,361\,53(53)$ from [56]. Other values are from references listed in the table and [3]. * from Ref. [54].

Species	I_{nuc}	A_{hfs} (MHz)	g_I	$ F, m_F\rangle$	B_∞ (G)	Δ (G)	a_{bg} (a_0)	Calculated μ_{cross}/μ_B	Ref.
^7Li	3/2	401.752	−0.001182	$ 1, +1\rangle$	736.8	−192.3	−24.5	0.94	[7]
^{23}Na	3/2	885.813	−0.000805	$ 1, +1\rangle$	907	1	63	0.91	[45]
^{39}K	3/2	230.859	−0.000142	$ 1, +1\rangle$	403.4	−52	−33	0.95	[46,51]
^{41}K	3/2	127.007	−0.000078	$ 1, −1\rangle$	51.34	0.3	60.54	0.07	[47]
^{85}Rb	5/2	1011.910	−0.000294	$ 2, −2\rangle$	155.4	11	−443	−0.57	[48]
^{87}Rb	3/2	3417.341	−0.000995	$ 1, +1\rangle$	1007.4	0.170	100.5	0.73	[32,52]
^{133}Cs	7/2	2298.157	−0.000399	$ 3, −3\rangle$	−11.7	28.7	1411.8	−0.75	[49,53]
^{52}Cr	0			$ 3, −3\rangle$	589.1	1.4	112	6*	[54]

In such a case, $\mu = \mu_B g_F m_F$. For higher fields, however, the Breit-Rabi formula is used for the ground states of alkali-metal atoms [50]:

$$E = \frac{-\Delta E_{hfs}}{2(2I+1)} + g_I \mu_B m_F B \pm \frac{\Delta E_{hfs}}{2} \left(1 + \frac{2m_F}{I+1/2} x + x^2 \right)^{1/2}, \quad (\text{B2})$$

where $m_F = m_I \pm 1/2$, $\Delta E_{hfs} = A_{hfs}(I+1/2)$ is the hyperfine splitting, $x = \frac{g \mu_B B}{\Delta E_{hfs}}$, and $g = g_J - g_I$.

The magnetic dipole moment is simply the derivative of the energy with respect to the magnetic field, resulting in

$$\mu(B) = g_I \mu_B m_F \pm \frac{\frac{2m_F}{2I+1} + x}{2\left(1 + \frac{4m_F}{2I+1} x + x^2\right)^{1/2}} g \mu_B. \quad (\text{B3})$$

This is used to calculate the magnetic moment μ_{cross} at B where $a_s = 0$ of all the alkali-metal species (see Table III).

-
- [1] T. Lahaye, C. Menotti, L. Santos, M. Lewenstein, and T. Pfau, *Rep. Prog. Phys.* **72**, 126401 (2009).
- [2] M. Baranov, *Phys. Rep.* **464**, 71 (2008).
- [3] T. Köhler, K. Góral, and P. S. Julienne, *Rev. Mod. Phys.* **78**, 1311 (2006).
- [4] C. Chin, R. Grimm, P. Julienne, and E. Tiesinga, *Rev. Mod. Phys.* **82**, 1225 (2010).
- [5] J. Stuhler, A. Griesmaier, T. Koch, M. Fattori, T. Pfau, S. Giovanazzi, P. Pedri, and L. Santos, *Phys. Rev. Lett.* **95**, 150406 (2005).
- [6] T. Koch, T. Lahaye, J. Metz, B. Fröhlich, A. Griesmaier, and T. Pfau, *Nat. Phys.* **4**, 218 (2008).
- [7] S. E. Pollack, D. Dries, M. Junker, Y. P. Chen, T. A. Corcovilos, and R. G. Hulet, *Phys. Rev. Lett.* **102**, 090402 (2009).
- [8] M. Fattori, G. Roati, B. Deissler, C. D’Errico, M. Zaccanti, M. Jona-Lasinio, L. Santos, M. Inguscio, and G. Modugno, *Phys. Rev. Lett.* **101**, 190405 (2008).
- [9] M. Vengalattore, S. R. Leslie, J. Guzman, and D. M. Stamper-Kurn, *Phys. Rev. Lett.* **100**, 170403 (2008).
- [10] M. Lu, N. Q. Burdick, S. H. Youn, and B. L. Lev, *Phys. Rev. Lett.* **107**, 190401 (2011).
- [11] K. Aikawa, A. Frisch, M. Mark, S. Baier, A. Rietzler, R. Grimm, and F. Ferlaino, *Phys. Rev. Lett.* **108**, 210401 (2012).
- [12] S. Giovanazzi, A. Görlitz, and T. Pfau, *Phys. Rev. Lett.* **89**, 130401 (2002).
- [13] S. Ronen, D. C. E. Bortolotti, and J. L. Bohn, *Phys. Rev. Lett.* **98**, 030406 (2007).
- [14] R. M. Wilson, S. Ronen, and J. L. Bohn, *Phys. Rev. A* **80**, 023614 (2009).
- [15] S. Yi, L. You, and H. Pu, *Phys. Rev. Lett.* **93**, 040403 (2004).
- [16] S. Yi and H. Pu, *Phys. Rev. Lett.* **97**, 020401 (2006).
- [17] S. Yi and H. Pu, *Phys. Rev. A* **73**, 061602 (2006).
- [18] G. Gligorić, A. Maluckov, L. Hadžievski, and B. A. Malomed, *Phys. Rev. A* **79**, 053609 (2009).
- [19] M. Abad, M. Guilleumas, R. Mayol, M. Pi, and D. M. Jezek, *Phys. Rev. A* **79**, 063622 (2009).
- [20] S. Yi and L. You, *Phys. Rev. A* **63**, 053607 (2001).
- [21] T. Lahaye, T. Koch, B. Fröhlich, M. Fattori, J. Metz, A. Griesmaier, S. Giovanazzi, and T. Pfau, *Nature (London)* **448**, 672 (2007).
- [22] L. Santos, G. V. Shlyapnikov, P. Zoller, and M. Lewenstein, *Phys. Rev. Lett.* **85**, 1791 (2000).
- [23] W. Bao, Y. Cai, and H. Wang, *J. Comput. Phys.* **229**, 7874 (2010).
- [24] R. M. W. van Bijnen, N. G. Parker, S. J. J. M. F. Kokkelmans, A. M. Martin, and D. H. J. O’Dell, *Phys. Rev. A* **82**, 033612 (2010).
- [25] I. Sapina, T. Dahm, and N. Schopohl, *Phys. Rev. A* **82**, 053620 (2010).
- [26] V. M. Pérez-García, H. Michinel, J. I. Cirac, M. Lewenstein, and P. Zoller, *Phys. Rev. Lett.* **77**, 5320 (1996).
- [27] S. Yi and L. You, *Phys. Rev. A* **67**, 045601 (2003).
- [28] Electronic dipole-dipole interactions could be similarly characterized, but are not considered further in this paper.
- [29] We note that there are limitations to the Gaussian ansatz. For example, it does not account for biconcave structure predicted to occur in pancake traps. However, this is an issue more specific to the pancake traps and only in a certain region of interactions [13]. For most trap geometries (especially cigar traps) and properties studied in this paper, the Gaussian ansatz provides a good model to guide the experimental investigation of MDDI effects.
- [30] Typo in Refs. [20,27] corrected; S. Yi (private communication).
- [31] Code developed for this work was written in MATLAB, is available at www.physics.purdue.edu/quantum/MDDI and www.abeolson.com/physics/MDDI.html.
- [32] A. Marte, T. Volz, J. Schuster, S. Dürr, G. Rempe, E. G. M. van Kempen, and B. J. Verhaar, *Phys. Rev. Lett.* **89**, 283202 (2002).
- [33] C. Chin, V. Vuletic, A. J. Kerman, and S. Chu, *Phys. Rev. Lett.* **85**, 2717 (2000).
- [34] B. DeMarco, Ph.D. thesis, University of Colorado, 2001.
- [35] Y. Castin and R. Dum, *Phys. Rev. Lett.* **77**, 5315 (1996).
- [36] C. J. Pethick and H. Smith, *Bose-Einstein Condensation in Dilute Gases* (Cambridge University Press, Cambridge, UK, 2008).
- [37] C. A. Sackett, H. T. C. Stoof, and R. G. Hulet, *Phys. Rev. Lett.* **80**, 2031 (1998).
- [38] E. A. Donley, N. R. Claussen, S. L. Cornish, J. L. Roberts, E. A. Cornell, and C. E. Wieman, *Nature (London)* **412**, 295 (2001).
- [39] We have verified that delay collapse still occurs even when a_s is changed after a short delay (a few 100’s of μs , based on the typical experimental limitations on how quickly a_s can be varied) from the start of the TOF.
- [40] D. H. J. O’Dell, S. Giovanazzi, and C. Eberlein, *Phys. Rev. Lett.* **92**, 250401 (2004).
- [41] S. Giovanazzi, L. Santos, and T. Pfau, *Phys. Rev. A* **75**, 015604 (2007).
- [42] G. Bismut, B. Pasquiou, E. Maréchal, P. Pedri, L. Vernac, O. Gorceix, and B. Laburthe-Tolra, *Phys. Rev. Lett.* **105**, 040404 (2010).
- [43] S. E. Pollack, D. Dries, R. G. Hulet, K. M. F. Magalhães, E. A. L. Henn, E. R. F. Ramos, M. A. Caracanhas, and V. S. Bagnato, *Phys. Rev. A* **81**, 053627 (2010).

- [44] J. J. McClelland and J. L. Hanssen, *Phys. Rev. Lett.* **96**, 143005 (2006).
- [45] J. Stenger, S. Inouye, M. R. Andrews, H. J. Miesner, D. M. Stamper-Kurn, and W. Ketterle, *Phys. Rev. Lett.* **82**, 2422 (1999).
- [46] G. Roati, M. Zaccanti, C. D'Errico, J. Catani, M. Modugno, A. Simoni, M. Inguscio, and G. Modugno, *Phys. Rev. Lett.* **99**, 010403 (2007).
- [47] T. Kishimoto, J. Kobayashi, K. Noda, K. Aikawa, M. Ueda, and S. Inouye, *Phys. Rev. A* **79**, 031602 (2009).
- [48] S. T. Thompson, E. Hodby, and C. E. Wieman, *Phys. Rev. Lett.* **94**, 020401 (2005).
- [49] T. Weber, J. Herbig, M. Mark, H.-C. Nagerl, and R. Grimm, *Science* **299**, 232 (2003).
- [50] A. Corney, *Atomic and Laser Spectroscopy* (Oxford University Press, New York, 2006).
- [51] C. D'Errico, M. Zaccanti, M. Fattori, G. Roati, M. Inguscio, G. Modugno, and A. Simoni, *New J. Phys.* **9**, 223 (2007).
- [52] T. Volz, S. Dürr, S. Ernst, A. Marte, and G. Rempe, *Phys. Rev. A* **68**, 010702 (2003).
- [53] C. Chin, V. Vuletić, A. J. Kerman, S. Chu, E. Tiesinga, P. J. Leo, and C. J. Williams, *Phys. Rev. A* **70**, 032701 (2004).
- [54] J. Werner, A. Griesmaier, S. Hensler, J. Stuhler, T. Pfau, A. Simoni, and E. Tiesinga, *Phys. Rev. Lett.* **94**, 183201 (2005).
- [55] E. Arimondo, M. Inguscio, and P. Violino, *Rev. Mod. Phys.* **49**, 31 (1977).
- [56] P. J. Mohr, B. N. Taylor, and D. B. Newell, *Rev. Mod. Phys.* **84**, 1527 (2012).